Grainy multiverse

Bartłomiej Czech[*]

Department of Physics and Astronomy, University of British Columbia, 6224 Agricultural Road,
Vancouver, BC V6T 1Z1, Canada
(Received 10 June 2011; published 16 September 2011)

I consider a landscape containing three vacua and study the topology of global spacelike slices in eternal inflation. A discrete toy model, which generalizes the well-studied Mandelbrot model, reveals a rich phase structure. Novel phases include monochromatic tubular phases, which contain crossing curves of only one vacuum, and a democratic tubular phase, which contains crossing curves of all three types of vacua. I discuss the generalization to realistic landscapes consisting of many vacua. Generically, the system ends up in a grainy phase, which contains no crossing curves or surfaces and consists of packed regions of different vacua. Other topological phases arise on the scale of several generations of nucleations.

I. INTRODUCTION

The realization that string theory gives rise to a landscape of vacua opened the possibility that our Universe may be one of many nucleating bubbles expanding in an eternally inflating false vacuum [1,2]. The resulting picture poses a number of novel, conceptual problems: it is difficult to consistently define probabilities in eternal inflation (the cosmological measure problem) while the richness of the string landscape may pose an intrinsically insurmountable obstacle to phenomenological studies traceable to complexity theory [3]. This paper follows a suggestion of [4] to study one aspect of eternal inflation that is not afflicted by these difficulties, namely, the topology formed by the nucleating bubbles. One such study was carried out in [5], whose authors considered the topology and physics arising from a toy landscape containing two vacua, called white and black. This paper explores the effects of including more realistic, richer landscapes on the resulting multiverse topologies.

Classifying multiverses by topology is worthwhile for several reasons. First, it is well defined: I will be looking at topologies formed by nucleating and expanding bubbles on global spacelike slices of an inflating geometry, but as shown in [5], these topologies are independent of the choice of slicing. Second, topology allows one to study the global picture of eternal inflation without tackling the cosmological measure problem first. Third, it is robust in that it is not sensitive to details of bubble wall dynamics or other modeling peculiarities. Consequently, one can reliably resort to simplified models; in what follows I shall employ a discrete toy model due to Mandelbrot [6], which has been utilized previously in studies of eternal inflation, notably in [5]. Finally, the different topological phases of eternal inflation are characterized by different physics, much of which has not yet been fully understood.

In Sec. II I will briefly review the results of [5], who gave a physical characterization of the topological phases arising from a two-vacuum landscape. It is important to understand which of their findings carry over to more realistic, richer landscapes. As a first step in this direction, the present paper classifies the topologies arising from a landscape consisting of three vacua (called white, gray, and black) and discusses the many-vacuum limit qualitatively.

Topological phases of eternal inflation are differentiated by the existence of crossing curves and crossing surfaces [5]. Roughly, the system is said to possess white crossing curves if, at arbitrarily late times, any two arbitrarily far regions are connected by a curve wholly surrounded by the white vacuum. The definition of white crossing surfaces pertains to the existence at arbitrarily late times of surfaces entirely contained in the white region, whose boundary is arbitrarily large. Of course, the definitions for gray and black crossing curves and surfaces are analogous. Below I consistently use abbreviations WXC (white crossing curves) and WXS (white crossing surfaces) and their analogues for gray and black regions. As shown in [5], the existence of crossing curves and surfaces is independent of the choice of time slicing. Topological phases are defined over a parameter space, whose natural coordinates are the dimensionless nucleation rates of the bubbles of various colors, $\gamma = \Gamma H^{-4}$, where H^{-4} is the Hubble volume.

The main results of this paper are phase diagrams, which describe how multiverse topology varies over the space of landscape parameters. I consider explicitly a landscape containing three vacua and comment on the general case in the discussion in Sec. IV. In finding the phase diagrams, I employ the following strategy:

(1) Reduce the problem to its discrete version, a three-vacuum analogue of the Mandelbrot model [6,5]. This, along with a brief review of previous results, is the content of Sec. II.

(2) Identify sectors in the parameter space of the discrete model, whose phases can be inferred from the

[*]czech@phas.ubc.ca

phase structure of the well-studied two-vacuum Mandelbrot model. This is the content of Sec. III A.

(3) Assemble the full phase diagrams (Secs. III B and III C).

This methodology qualitatively determines the phase structure of the three-vacuum Mandelbrot model. Though one cannot lift it to continuous eternal inflation on a quantitative level, its qualitative lessons are robust and generalizable to more realistic landscapes. They suggest that rich landscapes generically give rise to a grainy phase, in which the geometry is packed with a hodgepodge of bubbles of various colors. Other topological phases arise on the scale of several generations of nucleations. More details are given in the discussion.

II. PRELIMINARIES

A. Setup

Consider a toy landscape consisting of three vacua: a false vacuum labeled white, an intermediate vacuum labeled gray, and a true vacuum labeled black. Assume that each vacuum has a non-negative cosmological constant. Start in an initial all-white universe. Bubbles of gray or black vacuum will form in the white region [7] with rates Γ^{wg} and Γ^{wb} and further, inside the nucleated gray regions, bubbles of black vacuum will appear with the rate Γ^{gb}. The Γ's compete with the rates of expansion of the parent white and gray vacua: when $\Gamma H^{-4} \sim 1$, the nucleated regions may percolate and form nontrivial topologies that are the subject of this paper. Because for "upward transitions" $\Gamma \ll H^4$ [8], I make the simplifying assumption of irreversibility: $\Gamma^{bg} = \Gamma^{bw} = \Gamma^{gw} = 0$. The goal is to understand the connectivity of gray and black regions on spatial slices of this system at late times, as functions of the dimensionless nucleation rate $\gamma^{wb} \equiv \Gamma^{wb} H_w^{-4}$ and its analogues γ^{wg} and γ^{gb}. Reference [5] showed that this question is well defined, because the topology of the regions filled with descendant vacua is independent of the choice of time slicing.

B. Topological phases of eternal inflation with two vacua

Reference [5] (see also [9]) studied the analogous problem for a landscape consisting of two vacua. They found four topological phases, distinguished by the presence or absence of white crossing surfaces, white crossing curves, and their black analogues (BXS and BXC). Formally, these objects are defined as follows. Consider a three-dimensional ball of constant comoving radius in the multiverse, and select two disjoint open sets on the sphere surrounding it. If at arbitrarily late times the ball possesses a curve entirely contained in regions of one vacuum (definite color, henceforth "monochromatic") that connects the two open sets, then we say that the multiverse contains

crossing curves of that color. Likewise, if at arbitrarily late times the ball contains a monochromatic surface that bisects it and screens the two open sets from one another, then we say that the multiverse contains crossing surfaces of that color.

The four topological phases identified by [5] are:

(1) *The black island phase*, which contains WXS but no BXC or BXS. The white regions inflate eternally. The black regions are isolated Coleman–De Luccia (CDL) bubbles filled with open Friedmann-Robertson-Walker (FRW) universes. They will occasionally collide with other similar bubbles so that their boundary will be a surface whose genus increases in time.

(2) *The tubular phase*, which contains crossing curves of both colors, but no crossing surfaces of either color. It is separated from the black island phase by a percolation transition studied in [10]. The genus of the boundary of the black region becomes infinite in finite time.

(3) *The white island phase* contains BXS but no WXC or WXS. It is characterized by a phenomenon, which [5] called "cracking," whereby the white regions become disconnected. The analysis of [5] indicates that this leads to a formation of singularities in black regions, which may be mimicked by Kruskal-Schwarzschild black holes. Thus, an observer in a black region does not see all the disconnected boundaries, but rather a finite number of boundaries demarcating white regions and a finite number of black hole horizons, each sized no larger than roughly the Hubble scale of the ancestor vacuum. A likely final fate of this geometry is a big crunch.

(4) *The aborted phase* is the phase in which the black vacuum entirely takes over the geometry while the white regions disappear. This takes place when $\Gamma^{wb} H_w^{-4} \gtrsim 1$.

Part of the motivation of this work is to check to what degree these findings extend to more general scenarios. As a first step toward that goal, I classify the phases of the three-vacuum Mandelbrot model by their topology, leaving their observational or theoretical characterization to future work.

C. Deriving the Mandelbrot model

Reference [5] motivated and illustrated their findings with a discrete model of eternal inflation. Variants of the same model were also used in prior studies of eternal inflation [4,10–12]. Because the present paper deals with a more complex situation, it is useful to carefully derive the correspondence between eternal inflation and its discrete analogue.

The interesting topology of eternal inflation arises from collisions between bubbles. A bubble of a descendant
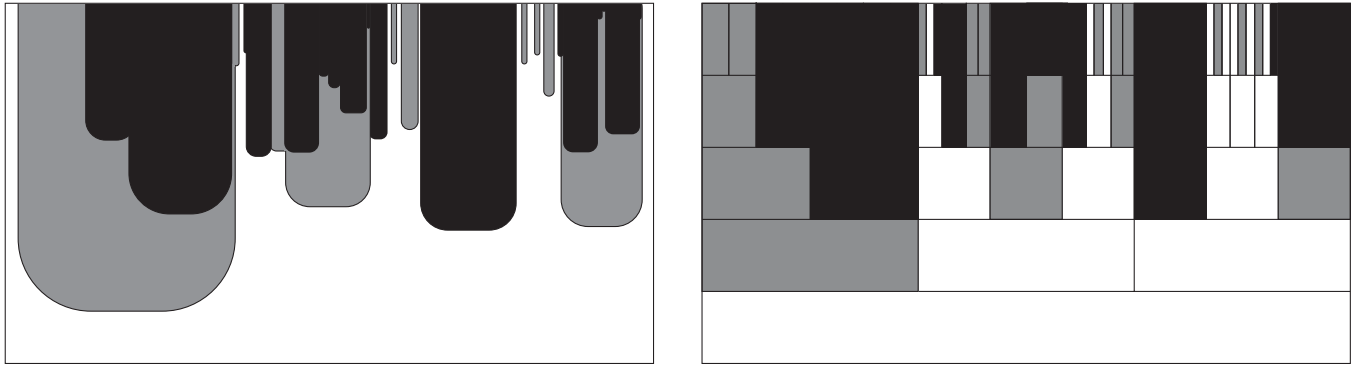
FIG. 1.   An example history of three-vacuum eternal inflation (left) and its discretized analogue (right). Horizontal axes correspond to comoving coordinates and span several initial Hubble lengths; the vertical axes mark time. The discrete evolution was emulated for $p_{wb} = 1/10$, $p_{wg} = 1/3$, $p_{gb} = 1/2$, $N_w = 3$, $N_g = 2$.

vacuum grows with a speed approaching the speed of light [7]. Meanwhile, the surrounding parent vacuum expands with a rate determined by its Hubble scale. Thus, in comoving coordinates of the parent vacuum, the bubble approaches a finite size given by the Hubble scale of the parent at the time of nucleation. Consequently, in cosmologies characterized by an accelerated expansion such as de Sitter, younger bubbles are smaller *when expressed in coming coordinates*. This is represented on the left of Fig. 1.

The goal is to study this system using a discrete model. How to discretize the left of Fig. 1? The first step is to chop the spatial slices of the geometry into discrete cells. The optimal cell size is the Hubble scale of the ancestor vacuum. With this choice, a nucleation event can be represented by filling the cell with the color of the nucleated vacuum. This is consistent, because each bubble quickly attains the parent Hubble size, though it never outgrows it. Furthermore, two bubbles are expected to collide if their nucleations are separated by distances smaller than the parent Hubble distance; otherwise their growth does not catch up with the expansion of the surrounding vacuum and they remain disconnected. This rule, which determines the connectivity of the bubbles, is naturally captured by setting the spatial unit cell to be Hubble sized.

The Hubble length in comoving coordinates is given by $1/\dot{a}(t)$, where $a(t)$ is the scale factor. If the expansion of the parent vacuum accelerates, $1/\dot{a}(t)$ is a decreasing function of time, which means that the Hubble length, when expressed in comoving coordinates, decreases. Thus, our unit spatial cells must in time be subdivided into smaller units. If one splits time into Δt intervals, each unit cell must be subdivided into

$$N = \frac{\dot{a}(t + \Delta t)}{\dot{a}(t)} \qquad (1)$$

subunits in each linear dimension. Thus, in three spatial dimensions, one subdivides each unit cell into N^3 subcells while in two dimensions the subdivision is into N^2 subunits. To take advantage of the convenience of a

discrete model, one should select Δt so that N is a natural number. In de Sitter space, this corresponds to setting Δt to be an order unity multiple of the Hubble time. The resulting model is known as the Mandelbrot model [6].

It remains to find a discrete analogue for the nucleation rate Γ, which defines the probability with which bubbles nucleate in a given four-volume. Our time intervals and spatial cells select a discrete unit of four-volume $H^{-3}\Delta t$ and, by extension, a dimensionless quantity $\Gamma H^{-3}\Delta t$. The probability with which the cells of the discrete model are colored black (or gray) must be a function of this quantity,

$$p = p(\Gamma H^{-3}\Delta t). \qquad (2)$$

Setting $p = \Gamma H^{-3}\Delta t$ is natural, but it is not the only reasonable choice. For example, the frequency of bubble nucleations in a given four-volume is given by the Poisson distribution; from that point of view, *not coloring* a discrete cell should happen with probability $1 - p \rightarrow \exp(-\Gamma H^{-3}\Delta t)$. The ambiguity in defining p shows that one should not attempt to derive quantitative results about eternal inflation from the Mandelbrot model. It is only a toy model of eternal inflation, which is expected to carry qualitative lessons.

I close this subsection by highlighting the definition of the Mandelbrot model in the form in which I will use it below. Begin with an infinite lattice of white cubes[1] and iterate the following procedure: subdivide each white cube into N_w^3 (N_w^2 in two dimensions) smaller cubes and color them gray with probability p_{wg} and black with probability p_{wb}; likewise, subdivide each gray cube into N_g^3 (N_g^2 in two dimensions) smaller cubes and color them black with probability p_{gb}. Take the limit of infinitely many iterations. Check for the existence of monochromatic curves that span an infinite distance (crossing curves) and for the existence of monochromatic two-surfaces that are unbounded in any

---

[1]I consider an infinite lattice instead of a single cube to eliminate tedious artifacts of an infrared cutoff.

direction (crossing surfaces). Note that $N_w \neq N_g$, because the expansions of the white and gray vacua accelerate at different rates [see Eq. (1)].

D. Topological phases of the Mandelbrot model with two vacua

The phase structure of the white-black Mandelbrot model in three dimensions was established in [13,14]. It mimics the phases of eternal inflation reviewed in Sec. II B. There is a black island phase (which contains WXS and no BXC), a tubular phase (which has crossing curves of both colors but no crossing surfaces), a white island phase (which contains BXS and no WXC), and the aborted phase (all black). The crossover value between the black island phase and the tubular phase is denoted p_s: after infinitely many iterations, BXC appear and WXS are eliminated if and only if $p \geq p_s$. In the tubular phase white and black regions each form connected networks of infinite genus. The critical value separating the tubular and the white island phase is p_c: after infinitely many iterations BXS appear and WXC are eliminated if and only if $p \geq p_c$. The phase transitions at p_s, p_c are first order.[2] Finally, in the aborted phase every region becomes all black after sufficiently many iterations. The onset of the aborted phase happens at $p_\varnothing(N) = 1 - N^{-3}$. The other transition points also depend on N. The exact forms of $p_s(N)$, $p_c(N)$ as functions of N are not known.

I will also study the two-dimensional Mandelbrot model, that is, one defined over a lattice of squares instead of cubes and in which cells are divided into N^2 units at each iteration. It is a toy model for studying the topology of gray and black regions on a spacelike two-dimensional surface, such as the wall surrounding a fiducial CDL bubble at a late time (compare with [15]). The two-dimensional model contains three phases: the black island phase (with WXC but no BXC), the white island phase (with BXC but no WXC), and the aborted phase. I will denote the boundary between the black island and the white island phases with $p_c(N)$. In two dimensions $p_\varnothing(N) = 1 - N^{-2}$.

III. PHASE DIAGRAMS

The goal is to understand the phase structure of three-vacuum eternal inflation (Sec. II A). I follow the strategy outlined in the introduction. The first step—a discretization of the system—was accomplished in Sec. II C. In this section the next two steps of the strategy are carried out. Section III A identifies special loci in the parameter space of the three-vacuum Mandelbrot model, whose topological phases can be inferred from the two-vacuum model and its

phase structure (reviewed in Sec. II D). These ingredients are then assembled to form the full phase diagrams of the three-vacuum Mandelbrot model in two (Sec. III B) and three dimensions (Sec. III C). I will discuss the extent to which these results can be lifted back to realistic, continuous eternal inflation in the discussion.

Before proceeding, some comments are in order. In the two-vacuum Mandelbrot model, the phases are characterized by whether at late enough times the white region contains crossing surfaces, crossing curves, or whether it is empty. The threshold values p_s, p_c, $p_\varnothing$ are functions of N, the number of subdivisions of white cells at each iteration. The technique is to lift these results to the three-vacuum model whenever possible. However, the three-vacuum Mandelbrot model contains two different values of N: N_w, which defines the number of subdivisions of white cells, and N_g, which is the number of subdivisions of gray cells. Consequently, the threshold values for the existence of white and gray crossing curves and surfaces, as well as for the white and gray regions to be empty, are different from one another. For this reason, I use superscripts to distinguish the critical probabilities governing the behavior of white and gray regions. For example, the probability of finding a WXS after infinitely many iterations vanishes if and only if $p_{wg} + p_{wb} \geq p_s^w$, but an analogous statement for gray regions, whatever its exact form, must depend on p_s^g and not p_s^w. Note that the parameter space of the three-vacuum Mandelbrot model is a product of a 1-simplex ($0 \leq p_{gb} \leq 1$) and a 2-simplex ($0 \leq p_{wg} + p_{wb} \leq 1$). I do not consider variations of N_w and N_g explicitly, because their effect is captured by shifting the phase boundaries p_s^w, p_s^g, p_c^w, p_c^g, $p_\varnothing^w$, $p_\varnothing^g$.

In all figures in this section, phase divisions that are known exactly [as functions of $p_s^w(N_w)$, etc.] are distinguished with the use of continuous lines from those which are known only qualitatively, represented by dashed lines. Dotted lines are auxiliary.

A. Ingredients

This subsection compiles the reasoning, by which results from the two-vacuum Mandelbrot model may be adapted to the three-vacuum case. Whenever possible, I list facts in indexed lists and use the same indices in the figures to mark the corresponding features of phase diagrams. I consider in turn the reasoning applicable to white, black, and gray regions.

White regions: For the purposes of studying the topology of the white regions, it is sufficient to focus on the projection of the parameter space onto the 2-simplex $0 \leq p_{wg} + p_{wb} \leq 1$, because p_{gb} plays no role here. On the projection, the different regimes are separated by downward-sloping 45° lines intersecting the p_{wb} axis at the critical values. The logic is that from the viewpoint of the white region, nucleations of the gray and black types are indistinguishable, so the boundary of the region

---

[2]At least in some models of eternal inflation, one would anticipate transitions that are second or higher order [15]. This disagreement is not relevant to the purposes of this paper, which are qualitative.
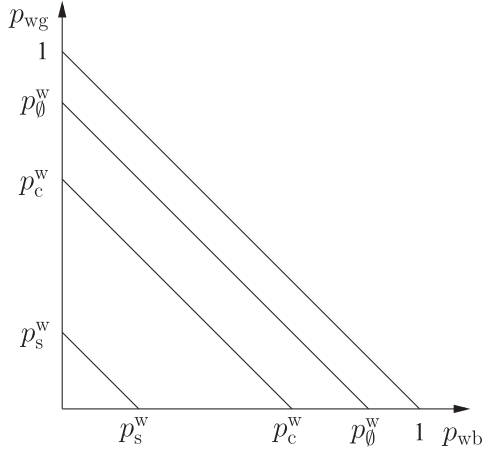
FIG. 2. Moving away from the origin, the successive regions contain WXS, WXC, white islands, and no white at all (the white-aborted phase). The points marked on the p_{wb} axis, p_s^w, p_c^w, $p_\emptyset^w$, are the locations of phase transitions in the two-vacuum Mandelbrot model.

containing WXS must be a level set of $p_{wb} + p_{wg}$. For example, since p_s^w marks the two-vacuum crossover from the black island (including WXS) to the tubular (including WXC) phase, the line $p_{wg} + p_{wb} = p_s^w$ demarcates the presence and absence of WXS. Analogous reasoning reveals the significance of parallel lines intersecting the values p_c^w and $p_\emptyset^w$, which separate the region containing only islands of white from that containing WXC and from the white-aborted phase. Facts about the white regions, which follow from the two-vacuum results, are summarized in Fig. 2.

Black regions: The topology of the black regions cannot be simply read off from the two-vacuum results, because it depends heavily on the value of p_{gb}. One may determine the boundaries between the topological phases of the black vacuum in the following steps, indexed in Fig. 3:

(1) Consider BXS and BXC. For positive p_{wg} and at $p_{gb} = 0$, their existence necessitates greater values of p_{wb} than in the two-vacuum system, because any white $\rightarrow$ gray transitions effectively lock those regions from ever becoming black. Therefore, a phase boundary at constant $p_{gb} = 0$ initially curves toward the diagonal $p_{wb} + p_{wg} = 1$, but becomes a straight line in the region $p_{wb} + p_{wg} \geq p_\emptyset^w$, because in the white-aborted phase and in the absence of gray $\rightarrow$ black transitions the relative abundance of gray and black can only depend on the ratio p_{wb}/p_{wg}.

(2) Consider the boundary between the phases containing black islands and BXC as p_{gb} increases. When $p_{gb} = p_s^g$, an intermediate formation of gray regions has no effect on the eventual formation of BXC, so that boundary is vertical (independent of p_{wg}). When $p_{gb} = p_c^g$, an analogous argument holds for the boundary between the phases containing BXC and BXS.

(3) If $p_{gb} \geq p_\emptyset^g$, then every gray region eventually becomes black and $p_{wb} + p_{wg}$ is again the relevant quantity for studying the topology of black. Point 3 of gray regions extends this conclusion to $p_{gb} \geq p_s^g$, p_c^g (for BXC and BXS, respectively).

(4) Finally for the aborted phase, in addition to the condition eliminating white regions, $p_{wb} + p_{wg} \geq p_\emptyset^w$, for positive p_{wg} one must also impose $p_{gb} \geq p_\emptyset^g$ to ensure that all the nucleating gray regions eventually become black. See also point 2 in gray regions.

Gray regions: The topology of the gray regions is determined by the following facts, which are indexed in Fig. 4:

(1) For $p_{gb} = 0$, the phase diagram is gray $\leftrightarrow$ black symmetric and Fig. 3 describes GXS and GXC, too.
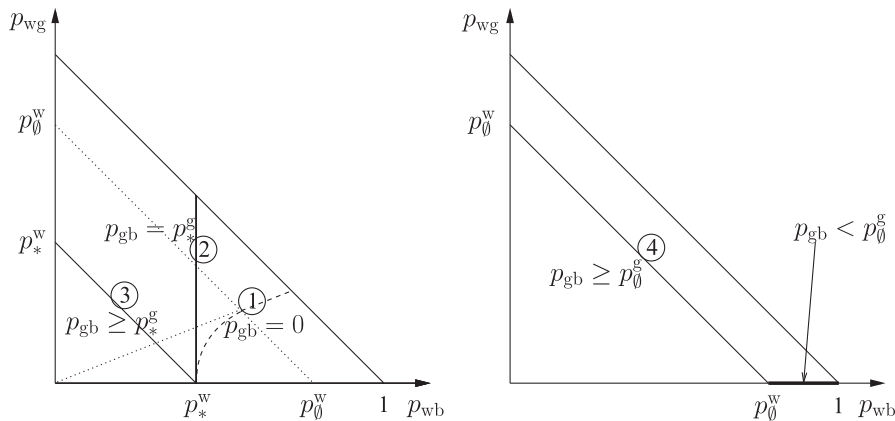

FIG. 3. The lines demarcating topological phases of black bubbles at constant p_{gb}. Left: the boundaries of the regions containing BXC ($p_*^w = p_s^w$) or BXS ($p_*^w = p_c^w$). Right: the aborted (all black) phase. The numbers refer to the observations listed in the text.
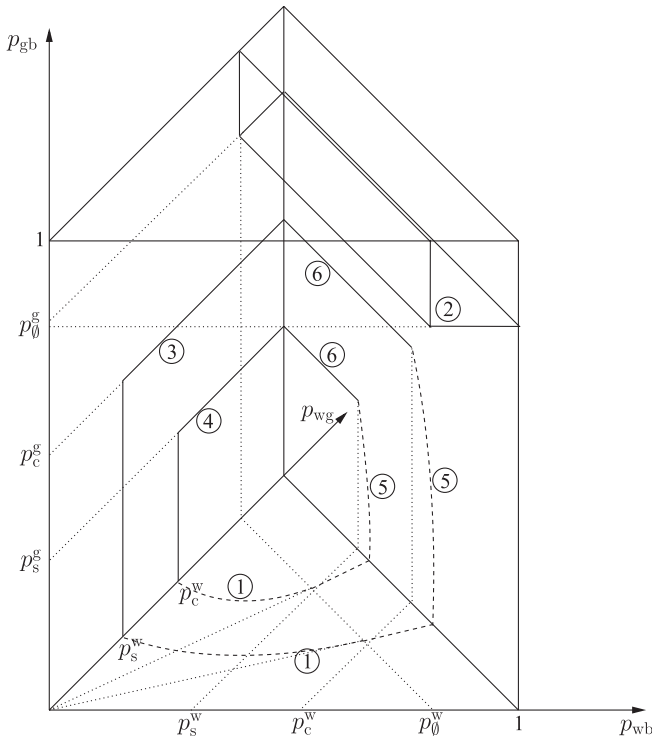
FIG. 4. The topological phases of the gray regions. Moving along the p_{wg} axis away from the origin, the successive domains contain gray islands, GXC, and GXS. The top wedge of the diagram is the aborted phase without any gray regions. The numbers refer to the observations listed in the text.

(2) For positive p_{wg} a necessary and sufficient condition for the system to contain no gray regions is $p_{wb} + p_{wg} \geq p_\emptyset^w$ and $p_{gb} \geq p_\emptyset^g$. To see this, note that the expected number of gray bubbles in one initial lattice cube after $i + 1$ iteration steps is

$$n_g(i+1)$$

$$= N_w^d p_{wg} \sum_{k=0}^{i} (N_w^d(1 - p_{wg} - p_{wb}))^k (N_g^d(1 - p_{gb}))^{i-k}$$

$$= N_w^d p_{wg} \frac{(N_w^d(1 - p_{wg} - p_{wb}))^{i+1} - (N_g^d(1 - p_{gb}))^{i+1}}{(N_w^d(1 - p_{wg} - p_{wb})) - (N_g^d(1 - p_{gb}))},$$

$$(3)$$

where k in the summation indexes the generation of gray bubbles that formed at the $(k + 1)$th step of the iteration. This expression cannot vanish unless both terms in the numerator go to zero individually, which is equivalent to the condition stated above. Physically, the requirement on $p_{wb} + p_{wg}$ is necessary because when it is violated, white regions continue to nucleate gray bubbles forever, which therefore persist arbitrarily late despite the fact

that each individual gray bubble eventually turns entirely black.

(3) Consider the regime $p_{wb} = 0$ and $p_{wg} \geq p_s^w$. If we ignore gray → black nucleations, the system develops GXC. One may then emulate the effect of a nonzero p_{gb} by studying an auxiliary two-vacuum (white vs nonwhite) Mandelbrot model, in which with probability p_{wg} one fills cells with gray cubes that already contain appropriate black structures inside them: black islands for $p_{gb} < p_s^g$, black crossing curves (spanning the length of the cube) for $p_s^g \leq p_{gb} < p_c^g$, or black crossing surfaces (spanning the cross section of the cube) for $p_{gb} \geq p_c^g$. Only the last possibility represents an obstruction to GXC, which shows that on $p_{wb} = 0$ and $p_{wg} \geq p_s^w$, the boundary of the gray tubular phase is $p_{gb} = p_c^g$. When $p_s^g \leq p_{gb} < p_c^g$, one obtains a gray tubular network of infinite genus forming GXC, which is percolated by a black tubular network of infinite genus containing BXC. This confirms the statement anticipated in point 3 of black regions — that BXC exist so long as $p_{wg} + p_{wb} \geq p_s^w$ and $p_{gb} \geq p_s^g$. An identical argument shows that BXS exist so long as $p_{wg} + p_{wb} \geq p_c^w$ and $p_{gb} \geq p_c^g$.

(4) One may similarly deduce the boundary of the phase containing GXS in the regime $p_{wb} = 0$ and $p_{wg} \geq p_c^w$. Again consider an auxiliary two-vacuum (white vs nonwhite) Mandelbrot model, in which with probability p_{wg} one fills cells with gray cubes that already contain the black structures dictated by p_{gb}. Now, as soon as $p_{gb} \geq p_s^g$, the BXC spanning the gray cubes preclude the survival of GXS. Thus, on $p_{wb} = 0$ and $p_{wg} \geq p_c^w$, the boundary of the phase containing GXS is $p_{gb} = p_s^g$.

(5) Consider the boundaries of the loci containing gray islands only, GXC, and GXS, and fix attention on the region $p_{wb} + p_{wg} \geq p_\emptyset^w$, where the system is all gray and black. By analogy with the two-vacuum system, these boundaries must coincide with phase boundaries demarcating domains with BXS, BXC, and black islands, respectively.

(6) Next, we noted in point 2 of Fig. 3 that these boundaries contain the points

$$(p_{wb}, p_{wg}, p_{gb}) = (p_*^w, 1 - p_*^w, p_*^g), \qquad (4)$$

with $p_* = p_c$, p_s, respectively. On the other hand, points 3 and 4 above dictate that the same boundaries contain the points $(0, 1, p_*^g)$. These two pairs of points are connected with straight lines.

B. Three vacua in two dimensions

It is interesting to study the topology of bubble collisions with the wall of a fiducial bubble. The Mandelbrot model in two dimensions is applicable to this problem.

Figure 5 is the phase diagram of the $d = 2$ Mandelbrot model, assembled from the observations of the preceding subsection.

Recall that in $d = 2$ vacua of a given color may be found in three phases, wherein regions of that color form crossing curves, isolated islands, or are absent altogether. Consequently, the phase diagram contains two boundaries of each color (vacuum). The domain of the diagram is the product of a 2-simplex ($0 \leq p_{wb} + p_{wg} \leq 1$) and a 1-simplex ($0 \leq p_{gb} \leq 1$).

The following seven phases are distinguished in the diagram in Fig. 5:

White	Gray	Black	White	Gray	Black	White	Gray	Black
WXC	islands	islands	islands	GXC	islands	∅	GXC	islands
			islands	islands	islands	∅	islands	BXC
			islands	islands	BXC	∅	∅	whole

Interesting is the emergence of a grainy phase, in which observers inside the fiducial bubble see on their sky three types of vacua, none of which percolates. Also note that the boundary between the white-aborted phases containing GXC and BXC is marked in Fig. 5 with a continuous line. Its exact location is fixed by symmetry.

C. Three vacua in three dimensions

The Mandelbrot model relevant for studying the topology of the inflating universe is in $d = 3$. Its phase diagram, assembled from facts listed in Sec. III A, is presented in Fig. 6. In three dimensions vacua of a given color may be found in four phases, in which regions of that color form crossing surfaces, crossing curves, isolated islands, or are absent altogether. Thus, the phase diagram contains three boundaries of each color (vacuum).

The point marked with a black dot in Fig. 6 is established as follows. *A priori*, there are three possibilities for where the boundaries of the phases containing BXC and GXC intersect on the plane $p_{gb} = 0$: below the line $p_{wb} + p_{wg} = p_c^w$, on that line, or above it. In the first case, the phase containing crossing curves of all three colors would
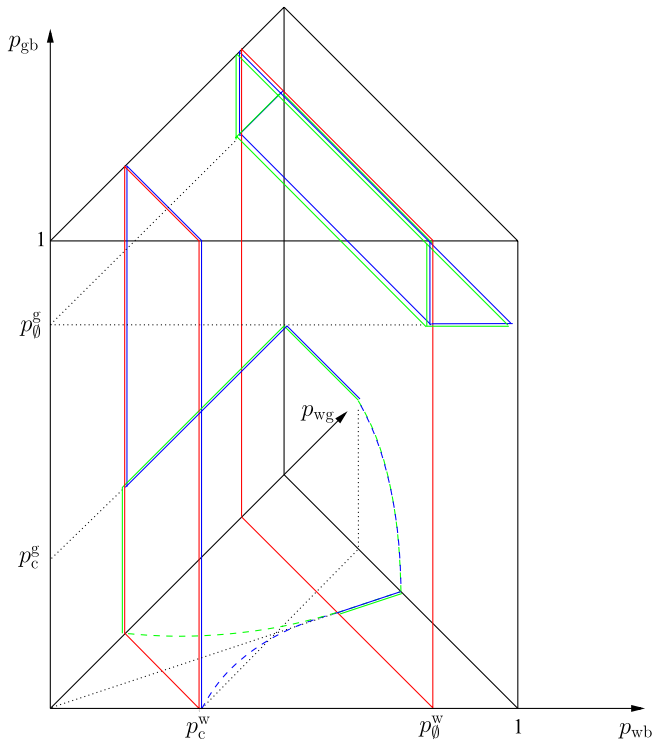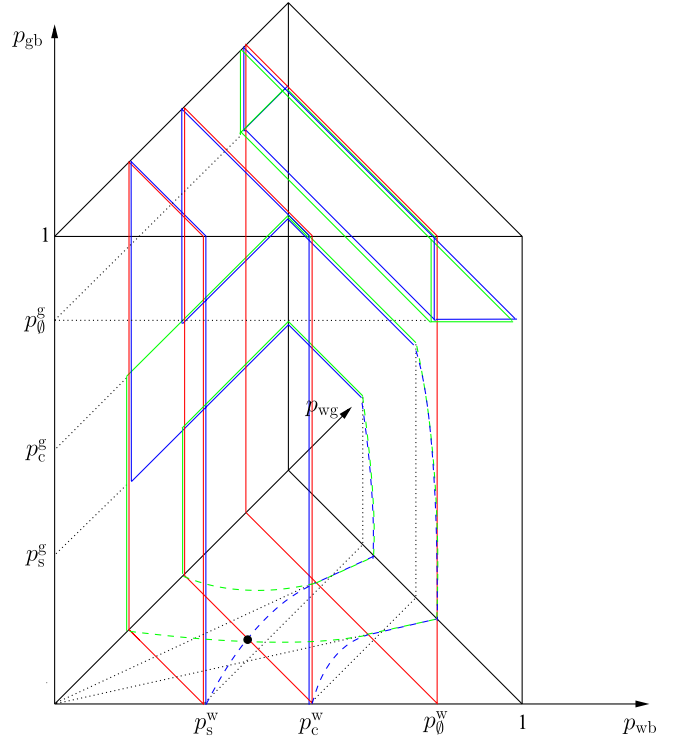

FIG. 5 (color online). The complete phase diagram of the $d = 2$ three-vacuum system. Boundaries of the topological phases of white regions are parallel planes, marked in red online; moving away from the origin, they contain WXC, white islands and no white at all (the aborted phase). Boundaries of the topological phases of gray regions are marked in green online; moving down from the top right, they contain no gray at all (the aborted phase), gray islands, and GXC. Boundaries of the topological phases of black regions are marked in blue online; moving down from the top right, they contain all space (the aborted phase), BXC, and black islands.

FIG. 6 (color online). The complete phase diagram of the $d = 3$ three-vacuum system. Boundaries of the topological phases of white regions are parallel planes, marked in red online; moving away from the origin, they contain WXS, WXC, white islands, and no white at all (the aborted phase). Boundaries of the topological phases of gray regions are marked in green online; moving down from the top right, they contain no gray at all (the aborted phase), gray islands, GXC, and GXS. Boundaries of the topological phases of black regions are marked in blue online; moving down from the top right, they contain all space (the aborted phase), BXS, BXC, and black islands. The black dot is explained in the text.

persist to $p_{gb} = 0$. This is unlikely, because point 3 of gray regions in Sec. III A identified nonzero p_{gb} as responsible for giving rise to that phase. I expect that the phase containing all three types of crossing curves persists only to some finite value of p_{gb}, but a formal proof of this statement is outside the scope of this paper. Next, if the boundaries of the phases with BXC and GXC met on $p_{gb} = 0$ above the line $p_{wb} + p_{wg} = p_c^w$, then another phase would exist, in which there would be no crossing curves of any color. But the absence of white crossing curves would imply that the combined gray and black regions form crossing surfaces, and the $d = 2$ two-vacuum Mandelbrot model reveals that any such a crossing surface must contain either a gray or a black crossing curve. Hence this possibility is also excluded. This implies that the phases with GXC and BXC meet on the plane $p_{gb} = 0$ precisely on the line $p_{wb} + p_{wg} = p_c^w$.

In summary, Fig. 6 contains the following 14 phases:

White	Gray	Black	White	Gray	Black	White	Gray	Black
WXS	islands	islands	islands	GXS	islands	∅	GXS	islands
WXC	GXC	BXC	islands	GXC	islands	∅	GXC	BXC
WXC	GXC	islands	islands	GXC	BXC	∅	islands	BXS
WXC	islands	BXC	islands	islands	BXC	∅	∅	whole
WXC	islands	islands	islands	islands	BXS			

The tubular phases arrange themselves in qualitatively novel ways. Recall that in the two-vacuum system crossing curves of both colors necessarily coexist. In contrast, the three-vacuum model contains three new, monochromatic tubular phases as well as a democratic tubular phase, which contains crossing curves of all three colors. The latter phase has an analogue for any number of vacua: the sequence of transition probabilities $p_s^i \leq p_{ii+1} < p_c^i$ (with all other p_{ij} set to zero) leads to a series of tubular networks, which are contained in one another in the order in which they nucleate.

IV. DISCUSSION

This paper determines the phase structure of the three-vacuum Mandelbrot model, which is a natural discrete toy model for studying the topology of three-vacuum eternal inflation. The model differs from those studied in [15–17] in that it was not designed in order to reveal quantitative results for a specific scenario. Instead, it illustrates the wealth of behaviors which can arise in a complex landscape containing many disorderly arranged minima: already with three vacua, the model has 14 topological phases. Some of them are qualitatively novel, especially the all-tubular phase containing crossing curves of all colors, one inside another. These new phases are not artifacts of the discreteness of the model or of limiting the landscape to three vacua. On the contrary, their emergence is a good starting point for imagining the phase structure of realistic eternal inflation.

It is useful to focus first on the three monochromatic tubular phases, which contain crossing curves of only one color. It is natural to conjecture that with four vacua, the three-dimensional Mandelbrot model develops a grainy phase devoid of any crossing curves. (Indeed, such a phase exists in the three-vacuum Mandelbrot model in two dimensions.) This phase should have an analogue in realistic eternal inflation, at least when the number of vacua is large enough. Furthermore, it is clear that as the number of vacua grows, the grainy phase takes up more and more volume of the phase diagram. This is because additional vacua take up space, so it is increasingly difficult to sustain extended structures of any color. At the same time, the conditions for the existence of crossing curves and surfaces becomes increasingly limiting: if a vacuum i decays to n descendants, crossing curves or surfaces require the smallness of a sum of n transition rates. Thus, one is led to the conclusion that as the number of vacua grows, the system is increasingly likely to find itself in the grainy phase, in which isolated bubbles of different vacua fill the geometry without forming crossing curves or surfaces.[3] Of course, this statement relies on the landscape being so large as to be essentially random; the grainy phase is generic in the ensemble of all large landscapes.

The grainy phase is physically interesting. It is characterized by continuous cracking: a process in which the boundary of the parent vacuum region becomes disconnected. Reference [5] concluded that in the two-vacuum model cracking leads to a formation of singularities in the surrounding descendant vacuum. In the many-vacuum case, however, every connected component of the parent vacuum region is surrounded by a collection of bubbles, each filled with a different vacuum. It is difficult to imagine surrounding such a structure with a homogeneous horizon. It would be exciting to study this scenario in detail.

If the grainy phase is generic, can we forget all about the 14 phases of the three-vacuum Mandelbrot model? Definitely not. Notice that Fig. 6 describes the existence of crossing curves and surfaces that span the infinite lattice that is the domain of the model. It does not tell us about curves which cross the interior of only a single bubble of a given color. One example of this is shown in Fig. 7: the range of parameters in the shaded region of the phase diagram gives rise to an arrangement containing gray islands, each of which is percolated by a black tubular network that could be called an intrabubble BXC.[4] The right panel of Fig. 7 presents a cartoon of the resulting geometry.

The emerging picture is the following. On a global slice the grainy phase is generic. The global geometry becomes partitioned into randomly colored solids, which do not form crossing curves. However, particular spheres can

---

[3]This finding should not be compared with the results of [16,17], who were interested in the number of collisions in the past light cone of a particular observer.

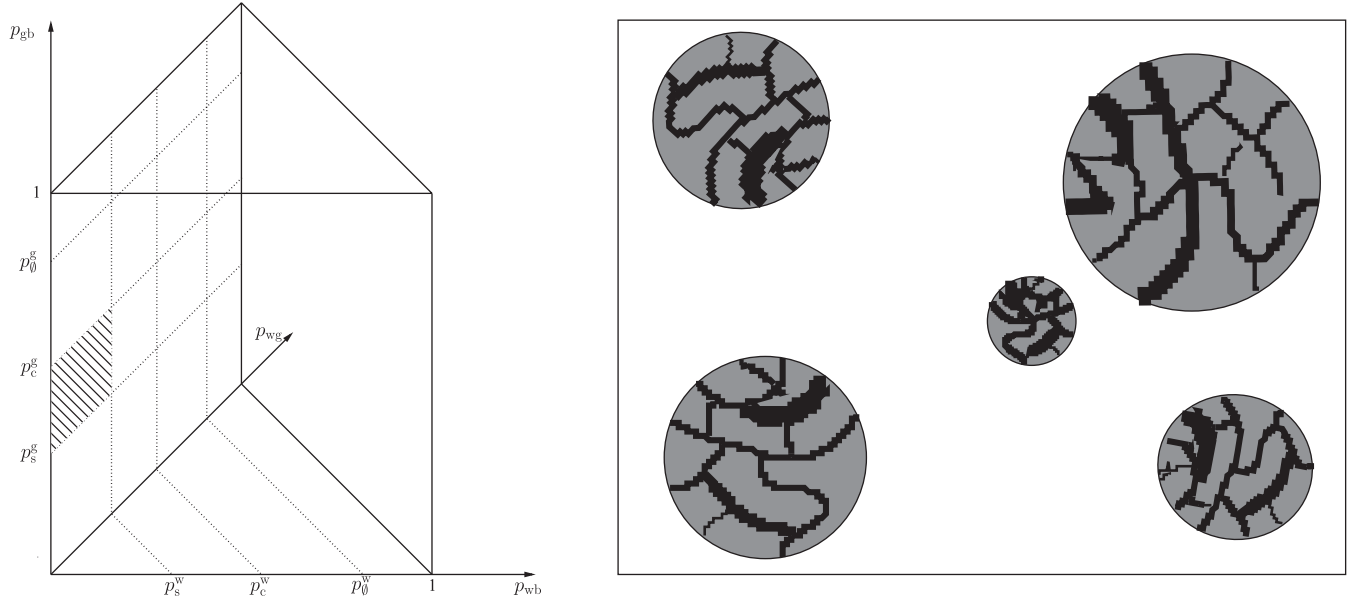[4]This example was also considered in Sec. VIII of [5].

FIG. 7.   The parameter range in phase space (left) that gives rise to global geometries containing gray islands, each of which is percolated by intrabubble BXC (right).

contain interesting topologies such as intrabubble crossing curves described in the last paragraph, or intrabubble crossing surfaces. Moreover, from Sec. III C we know that crossing curves can in principle be nested inside one another *ad infinitum*. Overall, the topological phases studied in the present paper and in [5] are also generic in eternal inflation. Their appearance, however, is likely limited to a scale of several generations, beyond which the multiverse finds itself in the grainy phase. It would be extremely interesting to derive this picture of eternal inflation from a theoretical framework such as [18].

ACKNOWLEDGMENTS

[1] R. Bousso and J. Polchinski, J. High Energy Phys. 06 (2000) 006.

[2] L. Susskind, arXiv:hep-th/0302219.

[3] F. Denef and M. R. Douglas, Ann. Phys. (N.Y.) **322**, 1096 (2007).

[4] S. Winitzki, Phys. Rev. D **65**, 083506 (2002).

[5] Y. Sekino, S. Shenker, and L. Susskind, Phys. Rev. D **81**, 123515 (2010).

[6] B. Mandelbrot, *The Fractal Geometry of Nature* (Freeman, New York 1983).

[7] S. R. Coleman and F. De Luccia, Phys. Rev. D **21**, 3305 (1980).

[8] K.-M. Lee and E. J. Weinberg, Phys. Rev. D **36**, 1088 (1987).

[9] R. Bousso, B. Freivogel, Y. Sekino, S. Shenker, L. Susskind, I. S. Yang, and C. P. Yeh, Phys. Rev. D **78**, 063538 (2008).

[10] A. H. Guth and E. J. Weinberg, Nucl. Phys. **B212**, 321 (1983).

[11] M. Aryal and A. Vilenkin, Phys. Lett. B **199**, 351 (1987).

[12] S. Winitzki, Phys. Rev. D **71**, 123507 (2005).

[13] J. T. Chayes, L. Chayes, and R. Durrett, Probab. Theory Relat. Fields **77**, 307 (1988).

[14] J. T. Chayes, L. Chayes, E. Grannan, and G. Swindle, Probab. Theory Relat. Fields **90**, 291 (1991).

[15] B. Freivogel and M. Kleban, J. High Energy Phys. 12 (2009) 019.

[16] J. Garriga, A. H. Guth, and A. Vilenkin, Phys. Rev. D **76**, 123512 (2007).

[17] B. Freivogel, M. Kleban, A. Nicolis, and K. Sigurdson, J. Cosmol. Astropart. Phys. 08 (2009) 036.

[18] B. Freivogel, Y. Sekino, L. Susskind, and C. P. Yeh, Phys. Rev. D **74**, 086003 (2006).